Black holes on FIRE: stellar feedback limits early feeding of galactic nuclei

Daniel Anglés-Alcázar,[1]* Claude-André Faucher-Giguère,[1] Eliot Quataert,[2] Philip F. Hopkins,[3] Robert Feldmann,[4] Paul Torrey,[5] Andrew Wetzel[3,6,7] and Dušan Kereš[8]

[1]*CIERA and Department of Physics and Astronomy, Northwestern University, 2145 Sheridan Road, Evanston, IL 60208, USA*
[2]*Department of Astronomy and Theoretical Astrophysics Center, University of California Berkeley, Berkeley, CA 94720, USA*
[3]*TAPIR, Mailcode 350-17, California Institute of Technology, Pasadena, CA 91125, USA*
[4]*Institute for Computational Science, University of Zurich, Zurich, CH-8057, Switzerland*
[5]*Department of Physics, MIT, 77 Massachusetts Avenue, Cambridge, MA 02139, USA*
[6]*The Observatories of the Carnegie Institution for Science, Pasadena, CA 91101, USA*
[7]*Department of Physics, University of California, Davis, CA 95616, USA*
[8]*Department of Physics, CASS, University of California at San Diego, 9500 Gilman Drive, La Jolla, CA 92093, USA*

ABSTRACT

We introduce massive black holes (BHs) in the Feedback In Realistic Environments (FIRE) project and perform high-resolution cosmological hydrodynamic simulations of quasar-mass haloes [$M_{halo}(z = 2) \approx 10^{12.5}\,M_\odot$] down to $z = 1$. These simulations model stellar feedback by supernovae, stellar winds and radiation, and BH growth using a gravitational torque-based prescription tied to the resolved properties of galactic nuclei. We do not include BH feedback. We show that early BH growth occurs through short ($\lesssim 1\,Myr$) accretion episodes that can reach or even exceed the Eddington rate. In this regime, BH growth is limited by bursty stellar feedback continuously evacuating gas from galactic nuclei, and BHs remain undermassive in low-mass galaxies relative to the local M_{BH}–M_{bulge} relation. BH growth is more efficient at later times, when the nuclear stellar potential retains a significant gas reservoir, star formation becomes less bursty and galaxies settle into a more ordered state. BHs rapidly converge on to the observed scaling relations when the host reaches $M_{bulge} \sim 10^{10}\,M_\odot$. We show that resolving the effects of stellar feedback on the gas supply in the inner $\sim 100\,pc$ of galaxies is necessary to accurately capture the growth of central BHs. Our simulations imply that bursty stellar feedback has important implications for BH–galaxy relations, AGN demographics and time variability, the formation of early quasars and massive BH mergers.

Key words: black hole physics – galaxies: active – galaxies: evolution – galaxies: formation – quasars: supermassive black holes – cosmology: theory.
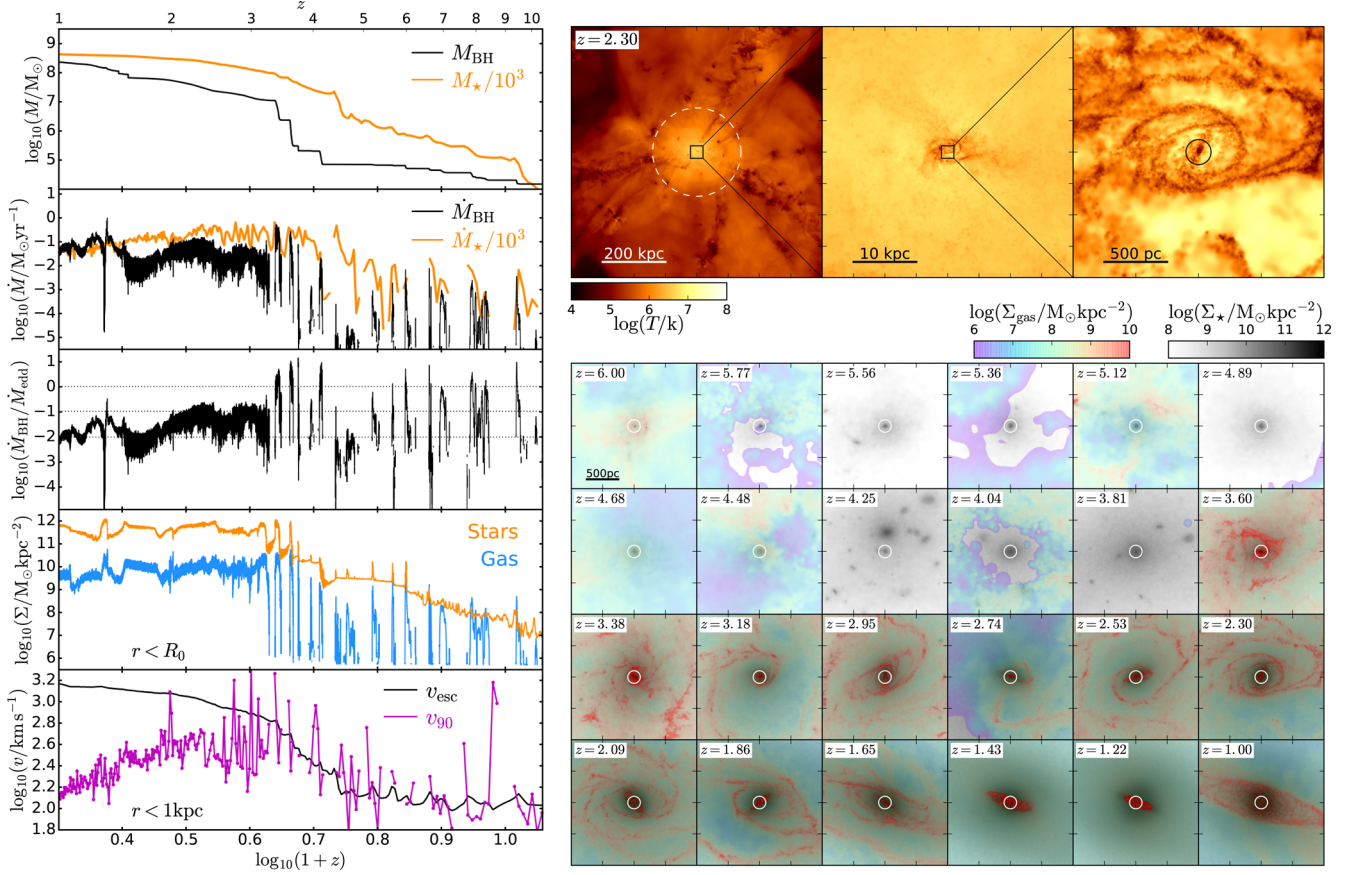
1 INTRODUCTION

The observed connection between galaxies and central massive black holes (BHs; e.g. Kormendy & Ho 2013; Heckman & Best 2014) poses significant challenges for galaxy formation models. Correlations between dynamical BH mass measurements and host galaxy properties in the local Universe (e.g. Häring & Rix 2004; Graham 2016; Savorgnan et al. 2016) have been interpreted as (1) a non-causal consequence of hierarchical merging (Peng 2007; Hirschmann et al. 2010; Jahnke & Macciò 2011), (2) the causal signature of self-regulation by BH feedback (e.g. Silk & Rees 1998; Di Matteo, Springel & Hernquist 2005; Murray, Quataert &

Thompson 2005; Hopkins et al. 2007) or (3) the result of a common gas supply for star formation and BH growth, regulated by gravitational torques (e.g. Kauffmann & Heckman 2009; Anglés-Alcázar, Özel & Davé 2013; Chen et al. 2013; Anglés-Alcázar et al. 2015, 2017a). Understanding nuclear fueling in a cosmological context is a crucial step towards uncovering the nature of BH–galaxy coevolution.

Recent progress from hydrodynamic simulations of galaxy formation has been limited by either resolution, interstellar medium (ISM) and stellar feedback physics, or the treatment of BH fueling. The Feedback In Realistic Environments (FIRE) cosmological 'zoom-in' simulations[1] (Hopkins et al. 2014, 2017) offer

---

* E-mail: anglesd@northwestern.edu

[1] http://fire.northwestern.edu

Figure 1. Left: evolution of the most massive BH in simulation A2 (a representative example). We show, from top to bottom: (1) BH mass, (2) accretion rate, (3) Eddington ratio, (4) gas/stellar mass surface density within the variable accretion radius $R_0 \lesssim 100$ pc and (5) the 90th percentile radial velocity of outflowing gas within 1 kpc (v_{90}) compared to the escape velocity at 1 kpc (v_{esc}). The top two panels also indicate the total stellar mass and SFR of the host galaxy. Top right: projected mass-weighted gas temperature maps at $z = 2.3$ on different scales centred on the main BH. The white dashed line indicates R_{vir} (left) and the black circle (right) corresponds to the central 100 pc. Bottom right: projected gas surface density (from purple to red) overlaid on top of the stellar mass surface density (background grey-scale); we show redshift evolution from $z = 6 \rightarrow 1$. The white circles indicate the central 100 pc. Length scales indicated on the panels are in physical units. At early times, Σ_{gas} fluctuates by more than three orders of magnitude owing to stellar feedback evacuating gas within the accretion radius; $\dot{M}_{BH}$ can reach the Eddington rate but only intermittently during $\lesssim 1$ Myr phases. More sustained BH growth begins at $z \sim 4$, when the stars dominate the gravitational potential and the nuclear gas content becomes more steady.

an ideal setting to investigate the evolution of massive BHs. By implementing stellar feedback processes on the scale of star-forming regions directly following stellar population synthesis models, the FIRE simulations reproduce a variety of galaxy (Hopkins et al. 2014; Ma et al. 2016; Feldmann et al. 2017) and CGM (Faucher-Giguère et al. 2015, 2016; Muratov et al. 2015; Hafen et al. 2017) observables. Here, we use high-resolution cosmological hydrodynamic simulations of quasar-mass haloes ($M_{halo} \approx 10^{12.5}$ M$_\odot$ at $z = 2$; e.g. White et al. 2012) from early times down to $z = 1$ to study the impact of stellar feedback on massive BH growth. Our simulations model the inhomogeneous, dynamic interstellar medium in the nuclear regions of galaxies ($\lesssim 100$ pc) while self-consistently capturing mass transport from cosmological gas infall down to galactic nuclei (Fig. 1, top right). We build on results from nuclear-scale simulations (Hopkins & Quataert 2010, 2011; Hopkins et al. 2016) to estimate the feeding rate of the BH accretion disc based on resolved galaxy properties on scales $\lesssim 100$ pc. Crucially, we model the inflow rate driven by gravitational torques induced by non-axisymmetric perturbations in the stellar potential, which represents a significant improvement over models based on Bondi accretion.

2 SIMULATIONS

We use the N-body+hydrodynamics code GIZMO[2] (Hopkins 2015) to re-simulate four haloes from the A series of MassiveFIRE galaxies presented in Feldmann et al. (2017), which did not include BH physics. This set of simulations covers a range of halo formation histories for halo mass $M_{halo} \approx 10^{12.5}$ M$_\odot$ at $z = 2$. Our new simulations use the updated FIRE-2 code (Hopkins et al. 2017), including the meshless finite mass (MFM) hydrodynamics solver and improvements to the accuracy of stellar feedback coupling algorithms, described therein. We assume a standard ΛCDM cosmology consistent with observational constraints (e.g. Planck Collaboration et al. 2016) and evolve haloes down to $z = 1$ with baryonic and dark matter particle masses $m_b = 3.3 \times 10^4$ M$_\odot$ and $m_{DM} = 1.7 \times 10^5$ M$_\odot$ and force softenings $\epsilon_{gas} = 0.7$ pc, $\epsilon_\star = 7$ pc, $\epsilon_{BH} = 7$ pc, and $\epsilon_{DM} = 57$ pc, where ϵ_{gas} is the minimum adaptive force softening for gas (identical to the kernel smoothing scale) and $\epsilon_\star$, ϵ_{BH} and ϵ_{DM} are fixed in physical units at $z < 9$. Additionally, we use the Milky Way-mass galaxy m12i from the FIRE-2 Latte

[2] http://www.tapir.caltech.edu/phopkins/Site/GIZMO.html

simulation suite (Wetzel et al. 2016) at three different resolution levels ($m_b = [7, 56, 450] \times 10^3 \, M_\odot$) for numerical convergence tests (these runs do not include BHs).

We treat BHs as individual collisionless particles that grow through accretion and mergers (Springel, Di Matteo & Hernquist 2005). We model accretion as $\dot{M}_{BH} = (1 - \eta) \dot{M}_{Torque}$, where $\eta = 0.1$, $\dot{M}_{Torque} \propto \epsilon_T f_d^{5/2} M_d R_0^{-3/2} M_{BH}^{1/6}$ (Hopkins & Quataert 2011, equation 65), and f_d and M_d are the mass fraction and total mass of the disc (stars and gas) within a radial aperture R_0 enclosing 256 gas elements. An upper limit of 140 pc (physical) is imposed on R_0 to avoid accreting distant gas. The ϵ_T pre-factor encapsulates uncertainties in processes that affect gas transport on unresolved scales (e.g. BH feedback). We set $\epsilon_T = 2.5$ to match the observed normalization of the M_{BH}–M_{bulge} relation at late times but ϵ_T could in principle vary in different regimes. We refer to Anglés-Alcázar et al. (2017a) for details of the numerical implementation, including the on-the-fly bulge-disc decomposition. BHs can exceed the Eddington rate ($\dot{M}_{edd}$) by up to a factor of 10, consistent with recent simulations of super-Eddington accretion (e.g. Jiang, Stone & Davis 2014). Our results are largely insensitive to this limit (Section 3.3).
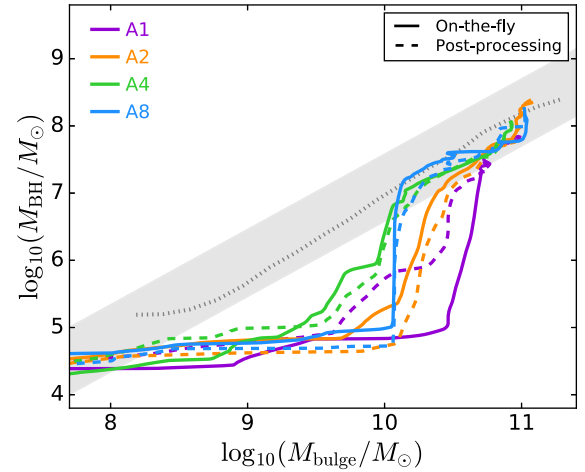
We introduce one BH seed with mass $M_{seed} = 1.4 \times 10^4 \, M_\odot$ at the location of the most bound star particle in haloes with stellar mass $M_\star^{fof} > 1000 \times M_{seed}$ using a friends-of-friends algorithm (e.g. Di Matteo et al. 2008). BH orbits are affected by dynamical friction, which would be underestimated owing to finite mass resolution. In order to more physically model BH dynamics, each BH is given an initial 'dynamical mass' $m_{BH} = 300 \times m_b \approx 60 \times m_{DM}$ independent of the physical M_{BH} set by accretion. Once M_{BH} reaches m_{BH}, both remain equal for the rest of the simulation. BH feedback is intentionally disabled to allow for a clean exploration of the impact of stellar feedback on BH growth. BH properties are saved at every time-step, yielding a time resolution in $\dot{M}_{BH}$ of up to 10^3 yr.

3 RESULTS

3.1 Representative black hole accretion history

Fig. 1 (left) shows the growth histories of the main galaxy in simulation A2 and its central BH. At early times, A2 experiences intense bursts of star formation, growing from $M_\star \sim 10^7 \rightarrow 10^{10} \, M_\odot$ in the redshift range $z = 10 \rightarrow 4$. During this early period, the total star formation rate (SFR) can reach $\dot{M}_\star \sim 10$–$400 \, M_\odot \, \mathrm{yr}^{-1}$. Stellar feedback drives large scale winds with 90th-percentile velocity $v_{90} \sim 10^2$–$10^3 \, \mathrm{km \, s}^{-1}$ (within 1 kpc), evacuating a large fraction of ISM gas and temporarily shutting down star formation (Muratov et al. 2015; Anglés-Alcázar et al. 2017b). Feedback-driven outflows/inflows cause significant radial stellar migration seen as fluctuations in $\Sigma_\star$ (El-Badry et al. 2016). As the galaxy grows to $M_\star > 10^{10} \, M_\odot$, star formation becomes less bursty and rapid outflow events become less frequent (e.g. Ma et al. 2017a). Sustained star formation at rates $\dot{M}_\star \sim 100 \, M_\odot \, \mathrm{yr}^{-1}$ grows the stellar mass to $M_\star = 4 \times 10^{11} \, M_\odot$ by $z = 1$ while maintaining a substantial nuclear gas reservoir ($\Sigma_{gas} \sim 10^{10} \, M_\odot \, \mathrm{kpc}^{-2}$).

Despite the rapid growth of the host galaxy, the central BH grows by less than one order of magnitude by $z = 4$. Early BH growth occurs through sporadic accretion episodes, reaching $\dot{M}_{BH} \sim 0.01 \, M_\odot \, \mathrm{yr}^{-1}$ when the nuclear gas surface density peaks at $\Sigma_{gas} \sim 10^8$–$10^9 \, M_\odot \, \mathrm{kpc}^{-2}$. BH accretion can reach or even exceed the Eddington rate during short phases ($\lesssim 1$ Myr), but the total mass accumulated is limited by the availability of gas to accrete over longer time-scales. At early times, Σ_{gas} fluctuates by more than

Figure 2. Evolutionary tracks of BHs and galaxies in the M_{BH}–M_{bulge} plane from early times down to $z = 1$ for the main halo in each simulation. Solid lines show simulation results while dashed lines correspond to post-processing calculations (see Section 3.2). The grey shaded area indicates 0.5 dex scatter in M_{BH} relative to the Häring & Rix (2004) relation. BHs are undermassive at early times and converge on to the scaling relation when their hosts reach $M_{bulge} \sim 10^{10} \, M_\odot$. This suppressed BH growth at early times is absent in lower resolution simulations with sub-grid ISM (grey dotted line; see Section 3.2).
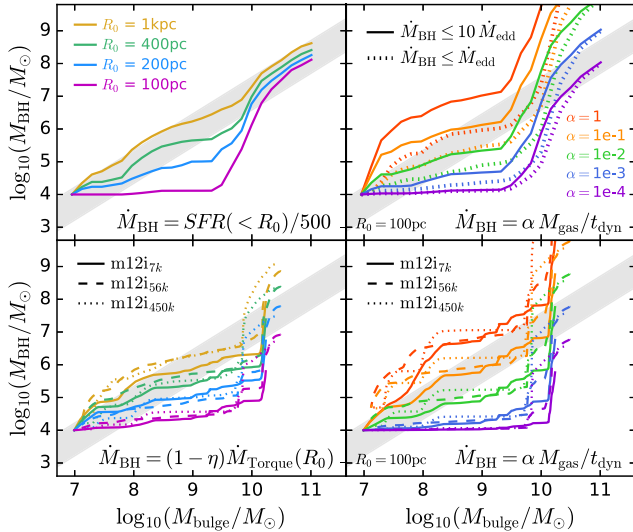
three orders of magnitude owing to bursty stellar feedback evacuating gas from the nucleus for $\sim$10–100 Myr intervals (e.g. Torrey et al. 2017). Efficient BH growth requires a sustained nuclear gas reservoir, only achieved at $z < 4$ when the stellar component dominates the gravitational potential and gas is more effectively retained in the nucleus (in other simulated haloes, efficient BH growth can be delayed until $z \sim 2$). Thumbnails in Fig. 1 (bottom right) show the evolution of the gas and stellar components in the central 2 kpc from $z = 6 \rightarrow 1$, illustrating the transition from (1) the irregular morphology, bursty star formation and highly dynamic conditions prevalent at early times to (2) the well-defined stellar potential, more steady star formation and long-lived nuclear gas disc enabling sustained BH growth at later times.

We find $\dot{M}_{BH} \sim 0.1 \, M_\odot \, \mathrm{yr}^{-1}$ frequently at $z < 4$, corresponding to a bolometric luminosity $L_{bol} \sim 6 \times 10^{44} \, \mathrm{erg \, s}^{-1}$ (for a 10 per cent radiative efficiency), while rare accretion episodes can reach $\dot{M}_{BH} \sim 1 \, M_\odot \, \mathrm{yr}^{-1}$. Our simulations thus predict that moderate luminosity active galactic nuclei (AGNs) at high redshift can be stochastically fueled and do not require major mergers events, in agreement with observations (e.g. Kocevski et al. 2012). The gas accreted by BHs during the late-time, more steady growth phase is heavily metal-enriched and a large fraction ($\gtrsim 50$ per cent) has been processed in earlier generations of stars, but not necessarily in the nucleus.

3.2 Black hole–host correlations

Fig. 2 shows the evolution of BHs and hosts in the M_{BH}–M_{bulge} plane from early times down to $z = 1$, where M_{bulge} is the bulge mass within the stellar effective radius (from a 3D kinematic decomposition; e.g. Anglés-Alcázar et al. 2014). As expected from Fig. 1, the central BH in galaxy A2 grows very little at early times, departing from the local scaling relation as the host galaxy grows. When the stellar bulge reaches $M_{bulge} \sim 10^{10} \, M_\odot$, the BH quickly converges on to the scaling relation. Similar tracks are seen for our A1, A4 and A8 simulations (the rapid increase in M_{BH} seen for A8 corresponds to a merger-triggered super-Eddington growth phase). The grey dotted

Figure 3. Top panels: evolutionary tracks in the M_{BH}–M_{bulge} plane averaged over our four quasar-mass haloes, where we compute BH growth in post-processing as $\dot{M}_{BH} = \dot{M}_*(R_0)/500$ for the SFR within different apertures $R_0 = 100\,\mathrm{pc}$–$1\,\mathrm{kpc}$ (left), and $\dot{M}_{BH} = \alpha\,M_{gas}/t_{dyn}$ for different α values, where $t_{dyn} \equiv (R_0^3/G M_{tot})^{1/2}$ and M_{tot} is the total mass within $R_0 = 100\,\mathrm{pc}$ (right). Bottom panels: Convergence tests for galaxy m12i at three resolution levels, where we compute $\dot{M}_{BH} = (1-\eta) \times \dot{M}_{Torque}$ for different R_0 (left) and $\dot{M}_{BH} = \alpha\,M_{gas}/t_{dyn}$ for $R_0 = 100\,\mathrm{pc}$ and different α values (right). We limit accretion to $\dot{M}_{BH} \leq 10\,\dot{M}_{edd}$ in all cases, except in the top right panel where we also show $\dot{M}_{BH} \leq \dot{M}_{edd}$ (dotted lines). The grey shaded area shows the Häring & Rix (2004) relation. Stellar feedback limits early BH growth when $\dot{M}_{BH}$ is tied to the gas content within ∼100 pc, but $\dot{M}_{BH}$ could be high enough to grow early massive BHs more quickly than in our fiducial calculations if α is temporarily elevated.

line indicates the median evolutionary track from the fiducial full-volume simulation of Anglés-Alcázar et al. (2017a), showing that the same accretion model does not yield slow early BH growth in lower resolution simulations with an effective sub-grid ISM model (Springel & Hernquist 2003), as was also found in Anglés-Alcázar et al. (2013, 2015).

The dashed lines in Fig. 2 show evolutionary tracks from post-processing calculations based on the same set of FIRE simulations, assuming that the BH is always located at the (dark matter + baryons) density centre of the halo computed with AHF (Knollmann & Knebe 2009). Following Anglés-Alcázar et al. (2015), we integrate $\dot{M}_{BH}$ using simulation snapshots available every ∼10–25 Myr, evaluating $\dot{M}_{Torque}$ for a variable aperture R_0 as in our on-the-fly calculation (Section 2). This analysis is insensitive to the exact definition of halo/galaxy centre and approximates very well our on-the-fly results. Since in our simulations BHs can move away from galaxy centres owing to dynamical interactions (e.g. Tremmel et al. 2015; Biernacki, Teyssier & Bleuler 2017), we conclude that BH dynamics is not the dominant factor responsible for the early suppression of BH growth.

3.3 Post-processing analysis

Fig. 3 shows several post-processing variations of our BH growth analysis. The top left panel shows M_{BH}–M_{bulge} evolutionary tracks down to $z = 1$ averaged over our four quasar-mass haloes assuming that $\dot{M}_{BH}$ is proportional to the SFR within a fixed physical radius at all times, $\dot{M}_{BH} = \dot{M}_*(R_0)/500$, where the normalization factor is the same for all R_0 (roughly the local observed M_{BH}/M_{bulge} ratio).

The characteristic transition in M_{BH} at $M_{bulge} \sim 10^{10}\,\mathrm{M}_\odot$ is recovered when the post-processing aperture is comparable to the on-the-fly calculations ($R_0 = 100\,\mathrm{pc}$). However, early BH growth is overestimated when using a larger aperture ($R_0 \geq 400\,\mathrm{pc}$) linking $\dot{M}_{BH}$ to the galaxy-scale gas reservoir. The top right panel of Fig. 3 shows average evolutionary tracks assuming that $\dot{M}_{BH}$ is proportional to the total gas mass within $R_0 = 100\,\mathrm{pc}$ accreted per dynamical time, $\dot{M}_{BH} = \alpha\,M_{gas}/t_{dyn}$, where we vary the normalization α and $\dot{M}_{BH}$ is limited to either $10\,\dot{M}_{edd}$ (solid lines) or $\dot{M}_{edd}$ (dotted lines). Predictions from this free-fall accretion estimator are in good agreement with $\dot{M}_{Torque}$ for $\alpha = 10^{-4}$–10^{-3}. The $\alpha = 1$ case represents the maximum BH fueling rate (for a given Eddington limit). Even in this case, the evolutionary tracks retain the characteristic transition from slower to faster growth at $M_{bulge} \sim 10^{10}\,\mathrm{M}_\odot$. None the less, for sufficiently high accretion efficiency per free-fall time at early times ($\alpha > 1$ per cent), there would be enough gas in galactic nuclei to rapidly grow BHs to the local M_{BH}–M_{bulge} relation.

The bottom left panel of Fig. 3 shows M_{BH}–M_{bulge} evolutionary tracks down to $z = 0$ for the Milky Way-mass galaxy m12i at three different resolution levels, where we integrate $\dot{M}_{BH} = (1-\eta) \times \dot{M}_{Torque}$ in post-processing for different R_0 (the m12i$_{7k}$ run reaches a mass resolution ∼5 × finer than our quasar-mass haloes). Small accretion radii ($R_0 \lesssim 200\,\mathrm{pc}$) produce evolutionary tracks in good agreement with Fig. 2, while larger apertures overestimate $\dot{M}_{BH}$. Despite a trend of earlier BH growth in lower-resolution calculations, evolutionary tracks are well converged for a wide range of R_0 and a factor 64× difference in mass resolution. We have also evolved our four quasar-mass haloes at 8× lower mass resolution and confirmed that our main conclusions are not sensitive to resolution. The bottom right panel of Fig. 3 shows the evolutionary tracks obtained for m12i evaluating $\dot{M}_{BH} = \alpha\,M_{gas}/t_{dyn}$ within $R_0 = 100\,\mathrm{pc}$, demonstrating good numerical convergence with resolution for different α values. The similar shape and normalization relative to the average evolutionary tracks for our quasar-mass haloes down to $z = 1$ (top right panel) suggest that the characteristic $\dot{M}_{BH}$ transition at $M_{bulge} \sim 10^{10}\,\mathrm{M}_\odot$ is independent of redshift, but a more comprehensive analysis will be needed to confirm this.

4 DISCUSSION AND CONCLUSIONS

We present the first cosmological simulations coupling the FIRE stellar feedback physics with a model for massive BH growth based on gravitational torques. By resolving the inner ∼100 pc of galaxies, we show that stellar feedback regulates the gas reservoir in galactic nuclei, which can severely limit early BH growth. Efficient BH growth begins when stars dominate the gravitational potential in the nucleus and star formation becomes less bursty, roughly when $M_{bulge} \sim 10^{10}\,\mathrm{M}_\odot$. At this stage, the galaxy centre becomes well defined and the escape velocity at 1 kpc exceeds that of stellar feedback-driven winds. This evolution in BH fueling mode roughly coincides with galaxy-scale transitions found previously in FIRE simulations, in which early bursty star formation transitions to long-lived gaseous discs with more time-steady star formation in more massive and lower-redshift galaxies (Muratov et al. 2015; Anglés-Alcázar et al. 2017b; Faucher-Giguère 2017; Hayward & Hopkins 2017; Ma et al. 2017a,b). Dwarf galaxies experience bursty star formation down to $z = 0$ (e.g. Anglés-Alcázar et al. 2017b), suggesting that BH growth will also be inefficient in low-redshift dwarfs. In such galaxies, inefficient BH growth may correlate with the formation of dark matter cores and stellar size fluctuations driven by stellar feedback (e.g. Chan et al. 2015; El-Badry et al. 2016).

We find that the early suppression of BH growth by stellar feedback is generic to models in which $\dot{M}_{BH}$ is tied to the nuclear gas content, provided that the effects of stellar feedback are resolved, suggesting that large-volume simulations that model $\dot{M}_{BH}$ based on the larger-scale ($\gtrsim 500\,\mathrm{pc}$) galactic gas reservoir will have difficulty correctly modelling BH growth. Recent simulations based on Bondi-like accretion and parametrized star-formation-driven kinetic winds (Costa et al. 2014) or delayed cooling thermal supernova feedback (Dubois et al. 2015; Bonoli et al. 2016; Bower et al. 2017; Habouzit, Volonteri & Dubois 2017; Prieto et al. 2017) also find suppressed $\dot{M}_{BH}$ in low-mass galaxies, in qualitative agreement with our results. However, Bondi accretion may inhibit the growth of low-mass BHs even in the presence of a continuous gas supply owing to the strong dependence on BH mass, $\dot{M}_{Bondi} \propto M_{BH}^2$ (e.g. Anglés-Alcázar et al. 2015), which may explain why some simulations predict suppressed $\dot{M}_{BH}$ despite having lower resolution than is needed to capture the stellar feedback effects identified here. In our simulations, most of the gas in the central $\sim$100 pc is cold and rotationally supported when BHs grow efficiently, justifying the use of the gravitational torque model instead of Bondi accretion.

Our fiducial simulations predict undermassive BHs in low-mass galaxies, in agreement with observations of the local M_{BH}–M_{bulge} relation (e.g. Graham & Scott 2013; Savorgnan et al. 2016), and substantial scatter in M_{BH} at $M_{bulge} \sim 10^{10}\,\mathrm{M}_\odot$ owing to rapid convergence on to the scaling relation once BHs start growing efficiently. In future work, it will be interesting to more systematically investigate the implications of stellar feedback for the growth of $z > 6$ quasars (e.g. Mortlock et al. 2011), overmassive relic BHs (e.g. McConnell et al. 2011), and M_{BH} measurements in active dwarfs (e.g. Jiang, Greene & Ho 2011; Reines, Greene & Geha 2013). The transition in BH fueling mode driven by stellar feedback also has direct implications for AGN demographics (e.g. Kauffmann et al. 2003; Aird, Coil & Georgakakis 2017) and for massive BH mergers and their observability by future gravitational wave missions, such as the Laser Interferometer Space Antenna (LISA; Amaro-Seoane et al. 2017). BHs are expected to be undermassive in low-mass satellites and experience reduced dynamical friction. The frequency and mass scale of massive BH mergers may thus be affected by stellar feedback.

After the early phase regulated by stellar feedback, BHs evolve along the M_{BH}–M_{bulge} relation without the need for large-scale AGN feedback self-regulation, in agreement with previous simulations with simpler subgrid ISM (Anglés-Alcázar et al. 2013, 2015). Simulations implementing gravitational torque-driven BH growth and feedback on $\sim$kpc scales indicate that large-scale AGN feedback may have a weak effect on the scaling relations, suppressing the growth of galaxies and BHs by a similar amount (Anglés-Alcázar et al. 2017a). None the less, BH feedback on smaller scales may play a significant role in determining $\dot{M}_{BH}$, which could affect some of our results. Future work should address the impact of AGN feedback in cosmological simulations implementing the stellar physics and dynamic range necessary to resolve galactic nuclei.

ACKNOWLEDGEMENTS

REFERENCES

Aird J., Coil A. L., Georgakakis A., 2017, MNRAS, preprint (arXiv:1705.01132)
Amaro-Seoane P. et al., 2017, preprint (arXiv:1702.00786)
Anglés-Alcázar D., Özel F., Davé R., 2013, ApJ, 770, 5
Anglés-Alcázar D., Davé R., Özel F., Oppenheimer B. D., 2014, ApJ, 782, 84
Anglés-Alcázar D., Özel F., Davé R., Katz N., Kollmeier J. A., Oppenheimer B. D., 2015, ApJ, 800, 127
Anglés-Alcázar D., Davé R., Faucher-Giguère C.-A., Özel F., Hopkins P. F., 2017a, MNRAS, 464, 2840
Anglés-Alcázar D., Faucher-Giguère C.-A., Kereš D., Hopkins P. F., Quataert E., Murray N., 2017b, MNRAS, 470, 4698
Biernacki P., Teyssier R., Bleuler A., 2017, MNRAS, 469, 295
Bonoli S., Mayer L., Kazantzidis S., Madau P., Bellovary J., Governato F., 2016, MNRAS, 459, 2603
Bower R. G., Schaye J., Frenk C. S., Theuns T., Schaller M., Crain R. A., McAlpine S., 2017, MNRAS, 465, 32
Chan T. K., Kereš D., Oñorbe J., Hopkins P. F., Muratov A. L., Faucher-Giguère C.-A., Quataert E., 2015, MNRAS, 454, 2981
Chen C., -T. J. et al., 2013, ApJ, 773, 3
Costa T., Sijacki D., Trenti M., Haehnelt M. G., 2014, MNRAS, 439, 2146
Di Matteo T., Springel V., Hernquist L., 2005, Nature, 433, 604
Di Matteo T., Colberg J., Springel V., Hernquist L., Sijacki D., 2008, ApJ, 676, 33
Dubois Y., Volonteri M., Silk J., Devriendt J., Slyz A., Teyssier R., 2015, MNRAS, 452, 1502
El-Badry K., Wetzel A., Geha M., Hopkins P. F., Kereš D., Chan T. K., Faucher-Giguère C.-A., 2016, ApJ, 820, 131
Faucher-Giguère C.-A., 2017, MNRAS, preprint (arXiv:1701.04824)
Faucher-Giguère C.-A., Hopkins P. F., Kereš D., Muratov A. L., Quataert E., Murray N., 2015, MNRAS, 449, 987
Faucher-Giguère C.-A., Feldmann R., Quataert E., Kereš D., Hopkins P. F., Murray N., 2016, MNRAS, 461, L32
Feldmann R., Quataert E., Hopkins P. F., Faucher-Giguère C.-A., Kereš D., 2017, MNRAS, 470, 1050
Graham A. W., 2016, Galaxy Bulges and Their Massive Black Holes: A Review. Springer International Publishing, Switzerland, p. 263
Graham A. W., Scott N., 2013, ApJ, 764, 151
Habouzit M., Volonteri M., Dubois Y., 2017, MNRAS, 468, 3935
Hafen Z. et al., 2017, MNRAS, 469, 2292
Häring N., Rix H.-W., 2004, ApJ, 604, L89
Hayward C. C., Hopkins P. F., 2017, MNRAS, 465, 1682
Heckman T. M., Best P. N., 2014, ARA&A, 52, 589
Hirschmann M., Khochfar S., Burkert A., Naab T., Genel S., Somerville R. S., 2010, MNRAS, 407, 1016
Hopkins P. F., 2015, MNRAS, 450, 53
Hopkins P. F., Quataert E., 2010, MNRAS, 407, 1529
Hopkins P. F., Quataert E., 2011, MNRAS, 415, 1027
Hopkins P. F., Hernquist L., Cox T. J., Robertson B., Krause E., 2007, ApJ, 669, 45

Hopkins P. F., Kereš D., Oñorbe J., Faucher-Giguère C.-A., Quataert E., Murray N., Bullock J. S., 2014, MNRAS, 445, 581

Hopkins P. F., Torrey P., Faucher-Giguère C.-A., Quataert E., Murray N., 2016, MNRAS, 458, 816

Hopkins P. F. et al., 2017, preprint (arXiv:1702.06148)

Jahnke K., Macciò A. V., 2011, ApJ, 734, 92

Jiang Y.-F., Greene J. E., Ho L. C., 2011, ApJ, 737, L45

Jiang Y.-F., Stone J. M., Davis S. W., 2014, ApJ, 796, 106

Kauffmann G., Heckman T. M., 2009, MNRAS, 397, 135

Kauffmann G. et al., 2003, MNRAS, 346, 1055

Knollmann S. R., Knebe A., 2009, ApJS, 182, 608

Kocevski D. D. et al., 2012, ApJ, 744, 148

Kormendy J., Ho L. C., 2013, ARA&A, 51, 511

Ma X., Hopkins P. F., Faucher-Giguère C.-A., Zolman N., Muratov A. L., Kereš D., Quataert E., 2016, MNRAS, 456, 2140

Ma X., Hopkins P. F., Feldmann R., Torrey P., Faucher-Giguère C.-A., Kereš D., 2017a, MNRAS, 466, 4780

Ma X., Hopkins P. F., Wetzel A. R., Kirby E. N., Anglés-Alcázar D., Faucher-Giguère C.-A., Kereš D., Quataert E., 2017b, MNRAS, 467, 2430

McConnell N. J., Ma C.-P., Gebhardt K., Wright S. A., Murphy J. D., Lauer T. R., Graham J. R., Richstone D. O., 2011, Nature, 480, 215

Mortlock D. J. et al., 2011, Nature, 474, 616

Muratov A. L., Kereš D., Faucher-Giguère C.-A., Hopkins P. F., Quataert E., Murray N., 2015, MNRAS, 454, 2691

Murray N., Quataert E., Thompson T. A., 2005, ApJ, 618, 569

Peng C. Y., 2007, ApJ, 671, 1098

Planck Collaboration et al., 2016, A&A, 594, A13

Prieto J., Escala A., Volonteri M., Dubois Y., 2017, ApJ, 836, 216

Reines A. E., Greene J. E., Geha M., 2013, ApJ, 775, 116

Savorgnan G. A. D., Graham A. W., Marconi A., Sani E., 2016, ApJ, 817, 21

Silk J., Rees M. J., 1998, A&A, 331, L1

Springel V., Hernquist L., 2003, MNRAS, 339, 289

Springel V., Di Matteo T., Hernquist L., 2005, MNRAS, 361, 776

Torrey P., Hopkins P. F., Faucher-Giguère C.-A., Vogelsberger M., Quataert E., Kereš D., Murray N., 2017, MNRAS, 467, 2301

Tremmel M., Governato F., Volonteri M., Quinn T. R., 2015, MNRAS, 451, 1868

Wetzel A. R., Hopkins P. F., Kim J.-h., Faucher-Giguère C.-A., Kereš D., Quataert E., 2016, ApJ, 827, L23

White M. et al., 2012, MNRAS, 424, 933

This paper has been typeset from a TEX/LATEX file prepared by the author.